The role of the serotonin 5-HT3 receptor in cortical development

Rigter, L.A.

Publication date
2010

Chapter 4

Alterations in apical dendrite bundling in the somatosensory cortex of 5-HT_{3A} receptor knockout mice

Laura A. Smit-Rigter, Wytse J. Wadman and
Johannes A. van Hooft

In preparation

Abstract

In the cerebral cortex of various species, apical dendrites of pyramidal neurons form clusters which extend through several layers of the cortex also known as dendritic bundles. Previously, it has been shown that 5-HT_{3A} receptor knockout mice show hypercomplex apical dendrites of cortical layer 2/3 pyramidal neurons, together with a reduction in reelin levels, a glycoprotein involved in cortical development. Other studies showed that in the mouse presubicular cortex, reelin is involved in the formation of vertical columnar structures and it has been hypothesized that in the presubicular cortex, the distribution of reelin-secreting Cajal-Retzius cells is related to the position of vertical columns. Here, we compare apical dendrite bundling in the somatosensory cortex of wildtype and 5-HT_{3A} receptor knockout mice. Using a microtubule associated protein (MAP) 2 immunostaining to visualize apical dendrites of pyramidal neurons, we compared dendritic bundle properties of wildtype and 5-HT_{3A} receptor knockout mice in tangential sections of the somatosensory cortex. A Voronoi tessellation was performed on immunostained tangential sections to determine the spatial organization of dendrites and dendritic bundles. A similar analysis was performed to investigate the distribution of reelin-positive Cajal-Retzius cells in wildtype and 5-HT_{3A} receptor knockout mice. In 5-HT_{3A} receptor knockout mice, dendritic bundle surface was larger compared to wildtype mice. Furthermore, we showed that while in both groups the distribution of dendritic bundles was regular, the distribution of reelin-positive Cajal-Retzius was random. Together with previously observed differences in dendritic complexity of cortical layer 2/3 pyramidal neurons and cortical reelin levels, these results suggest an important role for the 5-HT_3 receptor in determining the spatial organization of cortical connectivity in the mouse somatosensory cortex.

Chapter 4

Introduction

In various species and areas of the cerebral cortex, ascending apical dendrites of layer 5 pyramidal neurons and adjoining layer 2/3 pyramidal neurons are organized in clusters also referred to as dendritic bundles (Fleischhauer et al. 1972; Peters and Walsh 1972; Escobar et al. 1986; Peters and Kara 1987; White and Peters 1993; Lev and White 1997; Vercelli et al. 2004). Also in the mouse somatosensory cortex, dendritic bundles of ascending apical dendrites of pyramidal neurons through several layers of the cortex have been observed and their properties described (Escobar et al. 1986; White and Peters 1993). These dendritic bundles could form the basis of small functional units of vertically interconnected pyramidal and non pyramidal neurons called cortical modules, yet so far functional evidence is lacking for this hypothesis (Peters and Sethares 1996; Lev and White 1997; Rockland and Ichinohe 2004).

Recently, we showed that in the postnatal cortex, the serotonin 5-HT_3 receptor plays a pivotal role in the regulation of apical dendrite arborization of cortical layer 2/3 pyramidal neurons via a reelin dependent-pathway (Chameau et al. 2009). In mice lacking the 5-HT_{3A} receptor, we found a reduction in reelin levels and a hypercomplex dendritic tree of apical dendrites of cortical layer 2/3 pyramidal neurons (Chameau et al. 2009). In the developing cortex, the glycoprotein reelin is secreted by layer 1 Cajal-Retzius cells to act as a stop signal for migrating neurons and subsequently for ramifying dendrites of pyramidal neurons (D'Arcangelo et al. 1995; Chameau et al. 2009). In the mouse presubicular cortex, reelin is also involved in the formation of vertical columnar structures (Nishikawa et al. 2002; Janusonis et al. 2004). Based on observations in the presubicular cortex, it has been suggested that the distribution of Cajal-Retzius cells determines where vertical columns develop by forming reelin-rich cylindrical zones in which migrating neurons and their dendritic extensions do not settle (Nishikawa et al. 2002). Given these findings, we hypothesized that together with the alterations in reelin levels and dendritic complexity of cortical pyramidal neurons, mice lacking the 5-HT_{3A} receptor show alterations in dendritic bundle organization in the somatosensory cortex.

In the current study, we investigated the organization of dendritic bundles of ascending apical dendrites of pyramidal neurons in the somatosensory cortex of 5-HT_{3A} receptor knockout mice and compared them with controls. Dendritic bundle properties of wildtype and 5-HT_{3A} receptor knockout mice were compared in MAP-2 immunostained tangential sections from layer 3 of the somatosensory cortex.

In addition, we analyzed the distribution of reelin-positive Cajal-Retzius cells in tangential sections of the somatosensory cortex to find out whether the distribution of Cajal-Retzius cells is related to the position of dendritic bundles.

Materials and Methods

Animals and Immunohistochemistry

For these experiments, C57BL/6J and 5-HT_{3A} knockout mice (Zeitz et al. 2002) were used. From weaning (postnatal day 21) onwards, offspring was group-housed (4 per cage), with access to food and water *ad libitum* on a 12h/12h light dark cycle according to the guidelines of the ethical committee of the University of Amsterdam. At postnatal day (P) 4 and 14 and at 4 months of age, 3 to 8 mice per group were deeply anesthetized with a lethal i.p. dose of euthasol and perfused with 0.1M PBS, pH = 7.4, followed by 4% paraformaldehyde in PBS. Brains were dissected and after one hour of postfixation, hemispheres were separated and one hemisphere was flattened between two plastic foil-covered glass slides. After 24 hours of postfixation, both intact and flattened brains were kept in 0.25% paraformaldehyde in PBS. Forty micrometer thick coronal and tangential slices were cut on a vibroslicer (Leica VT1000S) and collected in PBS.

For the MAP-2 immunostaining, both coronal and tangential slices from adult mice were rinsed with PBS and endogenous peroxidases were removed with 3% H_2O_2 in PBS for 30 min, then slices were incubated in 0.1% triton-X and 5% NGS in PBS for 1 hour. Subsequently, slices were incubated overnight at 4˚C with 1:1500 MAP-2 HM-2 anti-mouse primary antibody (Sigma) in 0.1% triton-X and 5% NGS in PBS. The next day, slices were rinsed with PBS and incubated with 1:200 biotinylated sheep anti-mouse secondary antibody (Amersham) in 0.1% triton-X and 5% NGS in PBS for one hour, rinsed again with PBS, incubated with ABC (Vector labs UK) for 2 hours and visualized with a DAB (invitrogen USA) reaction. After 3 min, reaction was stopped and slices were mounted with moviol. The next day, images of the somatosensory cortex were captured using a Zeiss FS2 microscope with a 20x objective: dry Plan Neofluor 20x/0.50 and with Image Pro software.

For the reelin staining tangential slices from P4 and P14 mice were rinsed with PBS and incubated in 0.25% triton-X and 10% NGS in PBS for 1 hour. Subsequently, slices were incubated overnight at 4˚C with 1:1000 G-10 anti-mouse primary antibody (Abcam) in 0.25% triton-X and 5% NGS in PBS. The next day, slices were rinsed with PBS and incubated with 1:250 Alexa 488-conjungated goat anti-mouse (Molecular Probes) in 0.25% triton-X and 5% NGS in PBS for two hours. Again, slices were rinsed and mounted on glass slides with Vectashield (Vector labs UK).

Images were scanned on a confocal microscope (Zeiss LSM 510). Objective: dry Plan Neofluor 20x/0.75; filter: LP 560; beam splitter& HFT 488/543/633; laser HeNe 543nm.

For the reelin/MAP-2 double staining a 120 µm thick tangential slice of a P14 wildtype and 5-HT_{3A} receptor knockout mouse was cut and collected in PBS. To stain these slices the same procedure as for the reelin staining was followed, but in addition slices were incubated with 1:100 MAP-2 anti-rabbit primary antibody (Sigma) and 1:250 Alexa 568-conjungated goat anti-rabbit (Molecular Probes). Using the same confocal microscope, two images were scanned; one of the superficial reelin staining and one of the underlying MAP-2 staining. The two images were subsequently merged in ImageJ.

Dendritic bundle analysis

Tangential maps of 0.244 mm^2 through layer 3 (between 250-350 µm from the pial surface) were taken from sections immunostained for MAP-2. The mean dendrite diameter was determined as a mean of 20 apical dendrites per animal in layer 3 of the somatosensory cortex and all apical dendrites were located (x-y-coordinates). This analysis was performed using ImageJ software (Figure 1A). The location data were further analyzed with custom-made software written in MATLAB (MathWorks version 2007b).

Voronoi tessellation is a mathematical procedure that attributes a well defined surface to each dendrite by constructing a polygon around it where each side lies exactly in between two nearest neighbor dendrites (Figure 1B). The solution is unique and allows to calculate a mean surface around the dendrite and its standard deviation. The ratio between the two (sd/mean) is called the coefficient of variation (CV); its value is indicative for the nature of the spatial organization of the dendrites. A (Monte-Carlo style) study by Duyckaerts et al. (1994), demonstrated that a polygon surface CV value larger than 0.64 implies that the dendrites are clustered while a value less than 0.36 indicates a regularly distributed spatial organization of the dendrites. CV values that lie between 0.36 and 0.64 represent a randomly distributed spatial organization of the dendrites.

The Voronoi tessellation links each dendrite to a unique set of neighbors; for which inter-neighbor distances can now be calculated. Neighboring dendrites are considered to belong to the same bundle if the distance between them is smaller than a threshold value.

If this value is set too small, there will be no bundles and when it is set too high, they all belong to a single bundle. The relation between threshold (range 3.5 to 7.5 µm) and calculated bundle density (Figure 1C) shows an optimum between 4.5 and 6 µm. This relation was similar for wildtype and 5-HT_{3A} receptor knockout mice and for the rest of the study we choose a fixed threshold of 5.5 µm to define bundles. In addition, a bundle needed to consist of at least three dendrites in order to qualify as a bundle (Figure 1D).

Once a bundle was defined its location (x_b, y_b) was defined by its center of gravity: $x_b = \Sigma x_i$ and $y_b = \Sigma y_i$ over all dendrites in the bundle. Bundle surface was calculated in two different ways: 1) as the surface of the polygon that connects all dendrites continuously (see inset Figure 1D) or 2) as the surface of the polygon with the smallest circumference that includes all dendrites (see other bundles Figure 1D). The first measure was systematically 0.69 of the second one. We therefore present here only the second one (see Figure 5). With these definitions a set of parameters was calculated that characterizes the bundles and their organization. Finally a second Voronoi tessellation was performed on the bundle locations (x_b, y_b) allowing bundle organization quantification.

Analysis of the distribution of reelin-positive Cajal-Retzius cells:

In tangential sections of 0.21 mm^2 through layer 1 immunostained for reelin, the location of all reelin-positive Cajal-Retzius cells was determined, comparable to the determination of dendrite location, using ImageJ software. On these coordinates a Voronoi tessellation was performed in order to determine the spatial organization of the Cajal-Retzius cells.

Statistical Analysis:

All data are expressed as mean ± standard error of the mean (sem). Unless otherwise mentioned values were compared with Student's t-test. $p < 0.05$ was used to indicate a significant difference (in graphs indicated as *).

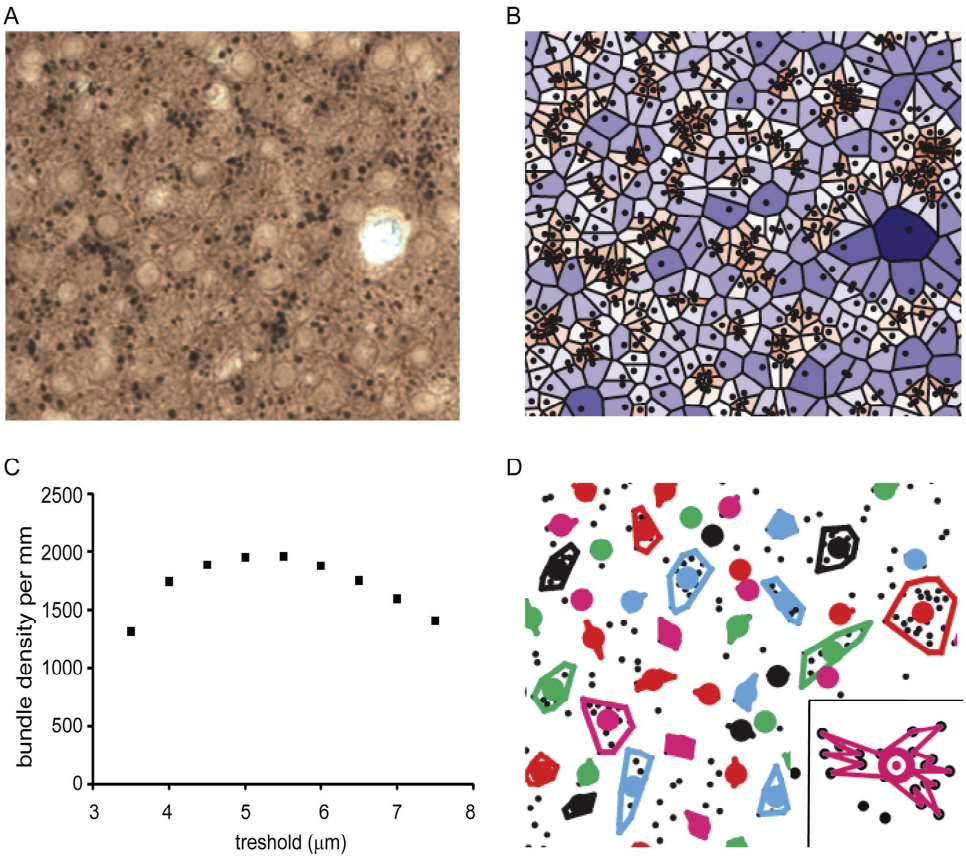

Figure 1. Quantitative analysis of dendritic bundles in the mouse somatosensory cortex. **(A)** Typical example of a MAP-2 immostained tangential section showing clusters of ascending apical dendrites of pyramidal neurons (black dots, see arrows). **(B)** Surface polygons as determined by the Voronoi tessellation (borders excluded), are marked by a color scale that indicates surface. Values range from small (blue) to large (red). **(C)** The mean dendritic bundle density per mm^2 in layer 3 of the somatosensory cortex of wildtype mice remains similar when the nearest neighbor distance threshold varies from 4.5 to 6 µm. **(D)** Using a nearest neighbor distance threshold of 5.5 µm and a minimum of 3 dendrites per bundle, bundles are now determined and bundle surface can be calculated in two different ways: 1) as the surface of the polygon with the smallest circumference that includes all dendrites (as shown in figure) or 2) as the surface of the polygon that connects all dendrites continuously (see inset). Coloured circles represent the location of the bundles (see methods).

Results

In both wildtype and 5-HT_{3A} receptor knockout mice, ascending apical dendrites of pyramidal neurons extend towards the pial surface in MAP-2 immunostained coronal sections of the somatosensory cortex (Figure 2). In these coronal sections of the somatosensory cortex, apical dendrites of pyramidal neurons from upper layers adjoin apical dendrites of pyramidal neurons from deeper layers to form clusters also known as dendritic bundles. A repetitive pattern of dendritic bundles of ascending apical dendrites through several layers of the cortex was visible, allowing quantification of the spatial organization of dendrites in MAP-2 immunostained tangential sections from layer 3 (located between 250-350 µm from the pial surface) of the somatosensory cortex (Figure 3A).

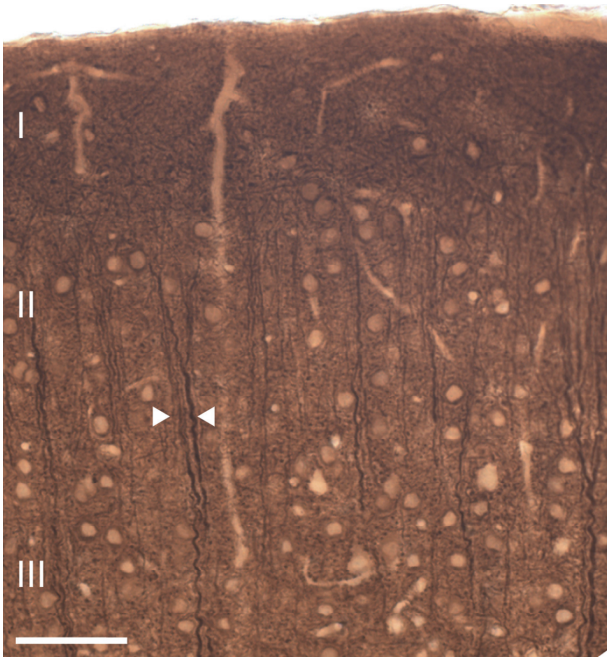

Figure 2. Ascending apical dendrites of cortical pyramidal neurons through several layers of the mouse somatosensory cortex form dendritic bundles. A typical example of a coronal section of the mouse somatosensory cortex showing MAP-2 immunostained dendritic bundles of ascending apical dendrites. Arrows indicate an example of a dendritic bundle. Scale bar 50 µm.

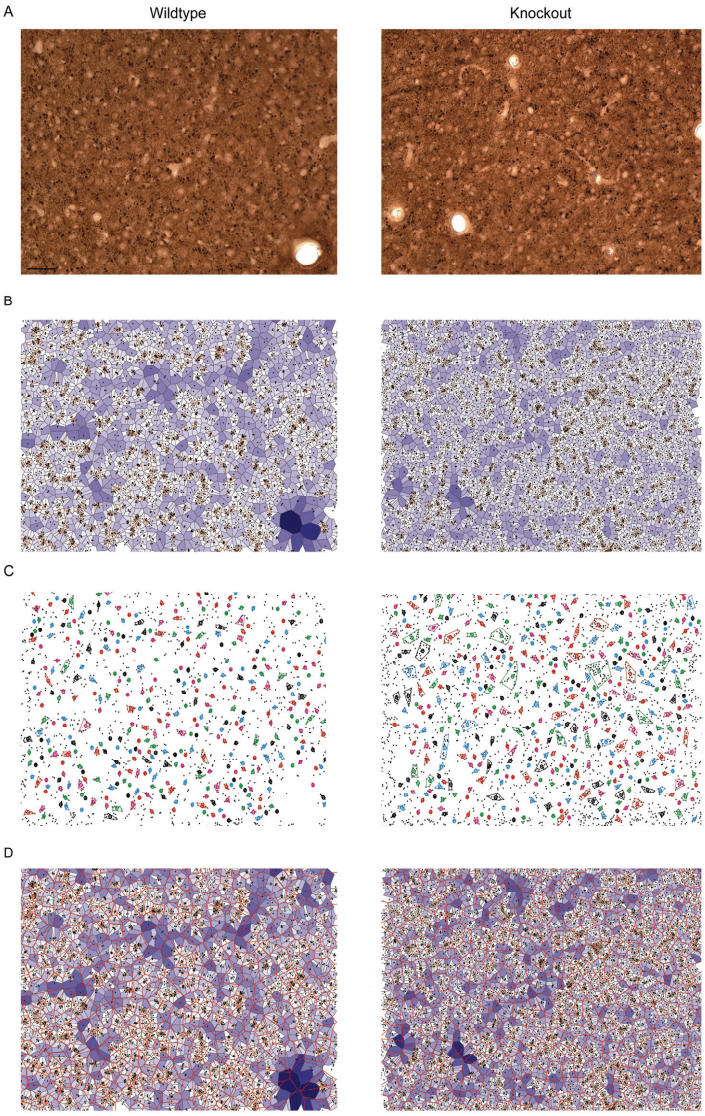

Figure 3. Quantitative analysis of dendritic bundles in the mouse somatosensory cortex of wildtype (left) and 5-HT$_{3A}$ receptor knockout mice (right). Typical examples of (**A**) MAP-2 immostained tangential sections show clusters of ascending apical dendrites of pyramidal neurons (seen from above as small black circles). (**B**) The polygons obtained using the Voronoi tessellation where the surface associated with each dendrite is indicated with a color scale from small (blue) to large (red). (**C**) Dendritic bundles as defined using a nearest neighbor threshold of 5.5 µm and a minimum of three dendrites in a bundle. Colored circles indicate the center of the bundles, drawn colored polygon indicates the outer circumference of the bundle and thus its size (**D**) Bundle polygons (red honeycomb structure) superimposed on the dendrite polygons. Scale bar 50 µm.

A Voronoi tessellation was performed on the collected dendritic coordinates to analyze the spatial organization of the apical dendrites in wildtype and 5-HT_{3A} receptor knockout mice (Figure 3B). The calculated polygon CV indicated that the distribution of apical dendrites in layer 3 of the somatosensory cortex of both wildtype and 5-HT_{3A} receptor knockout mice was clustered (WT; 0.67 ± 0.02, n = 8, KO; 0.64 ± 0.02, n = 5, n.s.) with no indication that there were differences between the groups.

Subsequently, dendritic bundles were defined using a nearest neighbor distance threshold of 5.5 µm and a minimum number of three dendrites in a bundle (Figure 3C). To determine the properties of the spatial distribution of the dendritic bundles, a second Voronoi tessellation was performed on the location coordinates (x_b,y_b) of the above defined bundles (Figure 3D). For wildtype and 5-HT_{3A} receptor knockout mice, the polygon CV was (WT; 0.36 ± 0.01, n = 8, KO; 0.34 ± 0.01, n = 5, n.s.) which for both situations is less or equal to 0.36 leading to the conclusion that the dendritic bundles are regularly organized (Duyckaerts et al., 1994). In addition, dendritic bundles are not differently organized in both groups of animals. Numerical properties of the dendritic bundles defined above for wildtype and 5-HT_{3A} receptor knockout mice are given in Table 1.

Table 1. Quantitative analysis of dendritic bundle properties in tangential sections from layer 3 of the somatosensory cortex of wildtype and 5-HT_{3A} receptor knockout mice.

	WT N=8	**KO N=5**
Average diameter dendrites (µm)	1.5 ± 0.01	1.5 ± 0.02
CV dendrites	0.67 ± 0.02	0.64 ± 0.02
Dendritic density (per mm2)	14232 ± 881	16504 ± 1233
CV dendritic bundles	0.36 ± 0.01	0.34 ± 0.01
Bundle density (per mm2)	1977 ± 103	1947 ± 76
Average dendritc bundle surface (µm2)	31 ± 4	56 ± 9 *
Average center-to-center distance (µm)	25.3 ± 0.6	25.6 ± 0.5
Number of dendrites per bundle	5.4 ± 0.2	6.7 ± 0.5

Analysis was performed on 0.244 mm^2 tangential sections from layer 3 immunostained for MAP-2 of 8 wildtype and 5 knockout mice (mean ± sem). CV = coefficient of variation. * indicates a significant difference between wildtype and KO group ($p<0.05$). Number of dendrites per bundle was tested using a Mann-Whitney test for non-parametric data.

Within the optical resolution the mean dendritic diameter was the same in both groups. Also the number of dendrites per mm^2, the number of dendritic bundles per mm^2, and mean center-to-center distance between neighboring bundles were not different in wildtype and 5-HT$_{3A}$ receptor knockout mice.

To analyze the distribution of the number of dendrites per bundle a histrogram was made (Figure 4). Although a tendency towards an increase in the number of dendrites per bundle in 5-HT$_{3A}$ receptor knockout mice was observed, the difference did not reach statistical significance. The analysis of the mean bundle surface of wildtype and 5-HT$_{3A}$ receptor knockout mice, calculated as described in the methods (Figure 5A), showed that bundle surface was almost twice as large in 5-HT$_{3A}$ receptor knockout mice than in wildtype mice (WT; 31 ± 4 μm^2, n = 8, KO; 57 ± 9 μm^2, n = 5, p = 0.013, Figure 5B).

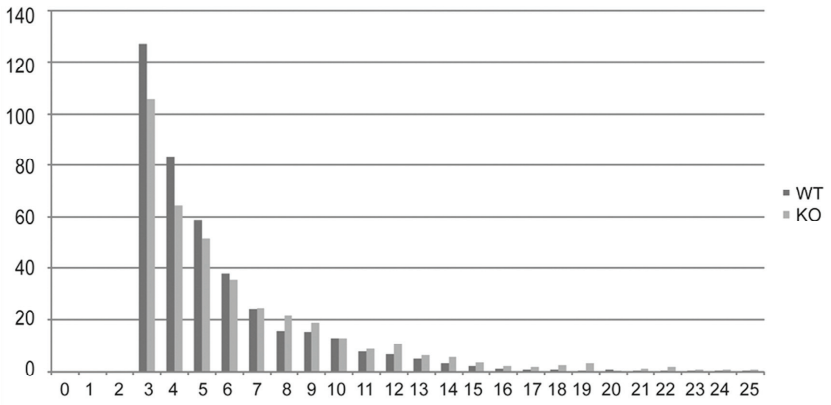

Figure 4. Histogram showing the distribution of the number of dendrites per bundle in tangential sections of the somatosensory cortex of wildtype and 5-HT$_{3A}$ receptor knockout mice.

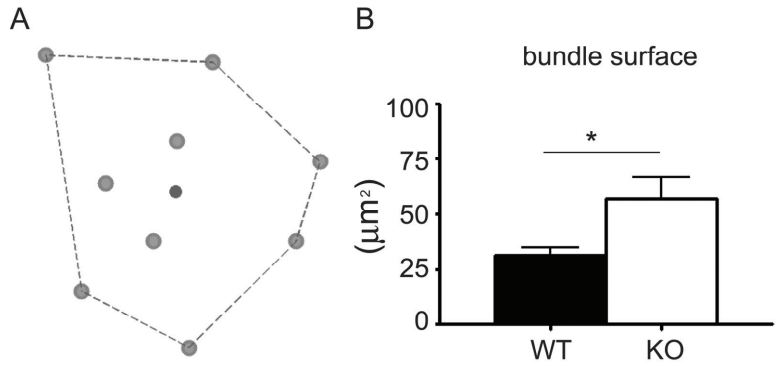

Figure 5. Surface of the dendritic bundles in layer 3 of the somatosensory cortex of wildtype and 5-HT_{3A} receptor knockout mice. (**A**) Bundle surface is determined by the polygon that connects dendrites in the bundle so that its circumference is the smallest one possible, while all dendrites in the bundle are localized within that polygon. The blue dot in the center represents the center of gravity (x_b,y_b). (**B**) The mean surface of layer 3 dendritic bundles in the somatosensory cortex is larger in 5-HT_{3A} receptor knockout mice than in wildtype mice ($p<0.05$).

At P4 and at P14, reelin-positive Cajal-Retzius cells could be observed in tangential sections from layer 1 of the somatosensory cortex of wildtype and 5-HT_{3A} receptor knockout mice (Figure 6A,B). A typical decrease in the number of reelin-positive Cajal-Retzius cells between P4 and P14 was found in wildtype (46%) as well as in 5-HT_{3A} receptor knockout mice (38%) (Table 2).

Table 2. Quantitative analysis of reelin-positive immunostained Cajal-Retzius cells in tangential sections of 0.21 mm^2 from layer 1 of the somatosensory cortex of wildtype and 5-HT_{3A} receptor KO mice.

	WT **N=3**	**KO** **N=4**
Age	**P4**	**P4**
CV Cajal-Retzius	0.40 ± 0.01	0.38 ± 0.02
CR cell density (per mm2)	598 ± 54	656 ± 7
Age	**P14**	**P14**
CV Cajal-Retzius	0.40 ± 0.02	0.35 ± 0.04
CR cell density (per mm2)	275 ± 9	251 ± 21

Analysis was performed on reelin layer 1 P4 and P14 tangential sections of 3 wildtype and 4 knockout mice. CV = coefficient of variation.

A Voronoi tessellation was performed on the location coordinates of Cajal-Retzius cells and the polygon CV was calculated as described above for dendrites and bundles. Analysis showed that for both P4 and P14 wildtype and 5-HT$_{3A}$ receptor knockout mice, the distribution of reelin-positive Cajal-Retzius cells was random, not clustered or regular and not different between the two genotypes. (P4: WT; 0.40 ± 0.01, n = 3, KO; 0.38 ± 0.02, n = 4, n.s.) (P14: WT; 0.40 ± 0.02, n = 3, KO; 0.35 ± 0.04, n = 3, n.s.) (Table 2).

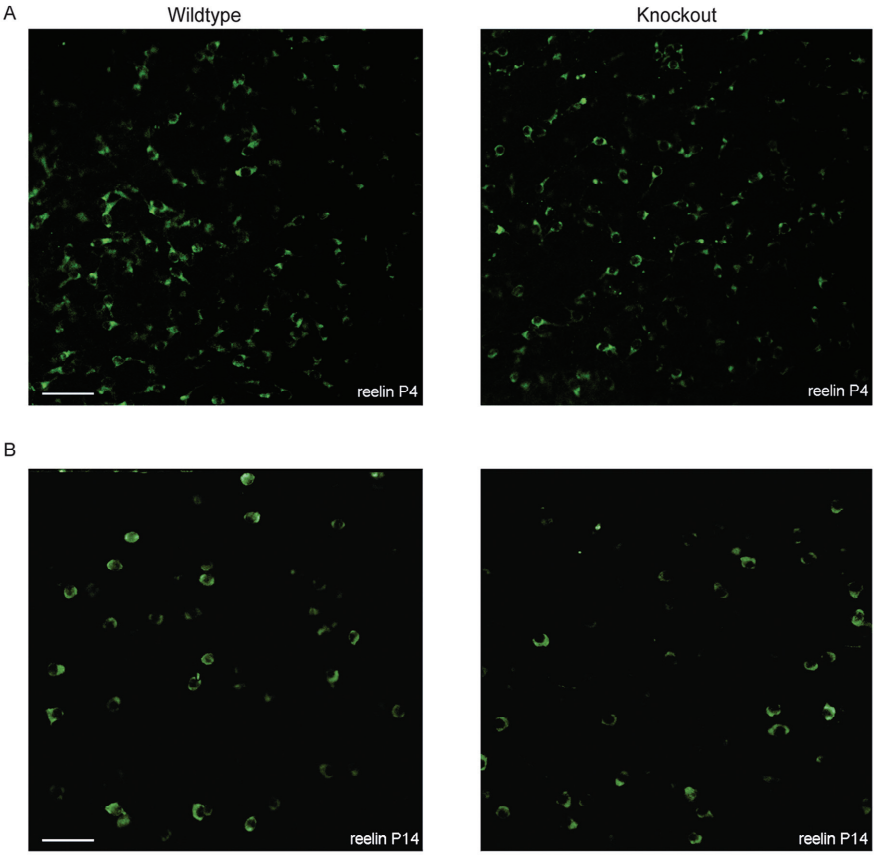

Figure 6. Tangential sections showing the distribution of reelin-positive Cajal-Retzius cells in the somatosensory cortex of both wildtype and 5-HT$_{3A}$ receptor knockout mice. Typical examples of reelin-positive Cajal-Retzius cells in P4 (**A**) and P14 (**B**) tangential sections of the somatosensory cortex of both wildtype and 5-HT$_{3A}$ receptor KO mice.

To have an idea about the relation between the spatial organization of Cajal-Retzius cells and dendritic bundles in the somatosensory cortex, a P14 tangential section (120 µm thick) of the somatosensory cortex of a wildtype and a 5-HT_{3A} receptor knockout mouse showing reelin-positive Cajal-Retzius cells superimposed on MAP-2 immunostained dendrites was made, yet no clear relation between the spatial distribution of Cajal-Retzius cells and dendritic bundles was observed (Figure 7B). However, a similar distribution of nearest neighbor distances for both dendritic bundles and Cajal-Retzius cells was observed (Figure 7A), suggesting a relation between the spatial organization of Cajal-Retzius cells and dendritic bundles in the somatosensory cortex.

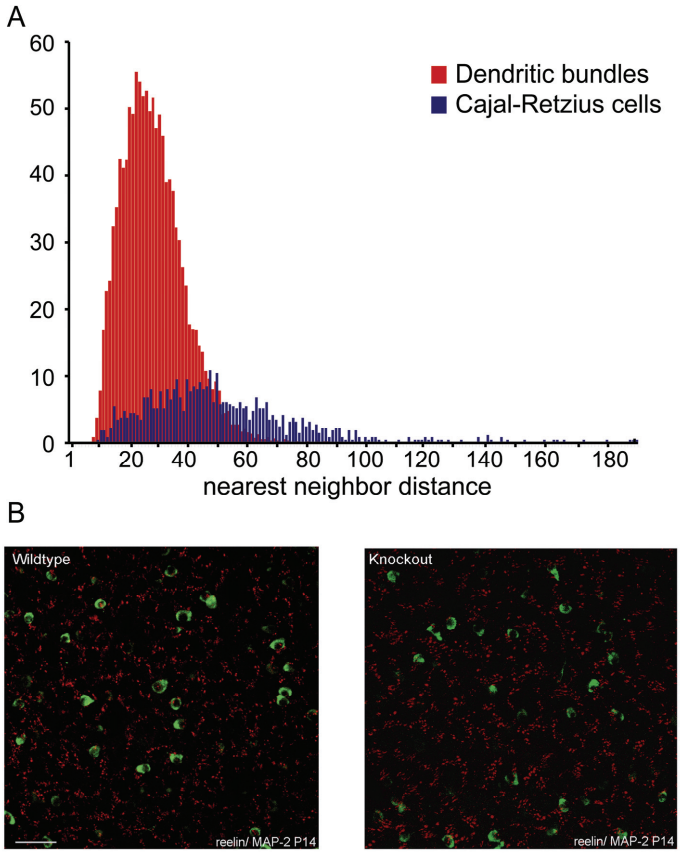

Figure 7. Distribution of reelin-positive Cajal-Retzius cells and dendritic bundles in the somatosensory cortex of wildtype mice. A P14 tangential section of the somatosensory cortex of a wildtype and 5-HT_{3A} receptor knockout mouse, showing the position of MAP-2 immunostained dendritic bundles and reelin-positive Cajal-Retzius cells. Scale bar 50 µm.

Discussion

In the current study, we quantified the spatial organization of ascending apical dendrites of pyramidal neurons which are organized in dendritic bundles in the somatosensory cortex of both wildtype and 5-HT_{3A} receptor knockout mice. In layer 3 tangential sections of the somatosensory cortex of 5-HT_{3A} receptor knockout mice, the average bundle surface is larger than in wildtype mice. Furthermore, we showed that in the somatosensory cortex of both wildtype and 5-HT_{3A} receptor knockout mice reelin-positive Cajal-Retzius cells are present in P4 and to a lesser extent in P14 tangential sections of layer 1 and that their distribution is random not regular or clustered.

To investigate dendritic bundle organization of both wildtype and 5-HT_{3A} receptor knockout mice we used a similar approach as Vercelli et al. (2004) to show that in both groups the distribution of layer 3 apical dendrites was clustered while the distribution of the dendritic bundles was regular. In concordance with a study of White and Peters (1993), who reported a bundle density of 1918 bundles per mm^2 and an average center-to-center distance between 22-25 µm in the mouse somatosensory cortex, here it was shown that dendritic bundles have a bundle density of 1978 bundles per mm^2 and mean center-to-center distance of 25 µm in wildtype mice.

It has been reported that in the postnatal cortex serotonin is the main excitatory drive for 5-HT_3 receptor-expressing Cajal-Retzius cells and that reelin controls dendritic maturation of cortical pyramidal neurons (Chameau et al. 2009). In neonatal mice of which the serotonergic innervation to these Cajal-Retzius cells was depleted, reelin levels were decreased and cortical column organization was disrupted (Janusonis et al. 2004). Based on the current observation that dendritic bundle surface was larger in 5-HT_{3A} receptor knockout mice, we suggest a relation between dendritic maturation and dendritic bundle formation in the somatosensory cortex and a role for reelin in regulating these events upon serotonergic activation of Cajal-Retzius cells.

According to the hypothesis of Nishikawa et al. (2002), the distribution of Cajal-Retzius cells determines where dendritic bundles develop by forming reelin-rich cylindrical zones in which migrating neurons and their dendritic extensions do not settle. In the current study, we wanted to test this hypothesis and investigated whether the distribution of Cajal-Retzius cells was related to the position of dendritic bundles.

In a P14 staining the relation between the position of Cajal-Retzius cells and dendritic bundles was not directly visible, yet it has to be mentioned that around this age most Cajal-Retzius cells have disappeared. Interestingly, the distributions of the nearest neighbor distances of the dendritic bundles and Cajal-Retzius cells, does support the idea of a relation between the distribution of Cajal-Retzius cells and the position of dendritic bundles. However, to ascertain whether a relation between the distribution of Cajal-Retzius cells and the position of dendritic bundles exists or not, additional studies should be performed at several stages of development and in particular during the first postnatal days when the Cajal-Retzius cell density is the highest. This is of particular importance in view of the fact that we based our analysis of the dendritic bundles on tissue from adult mice. In these studies the spatial organization of Cajal-Retzius cells and dendritic bundles needs to be compared in more detail and the average distance between Cajal-Retzius cells and dendritic bundles needs to be determined.

In the cortex, information processing occurs through local cortical microcircuits which show both interlaminar and intralaminar connections (Thomson and Bannister 2003). It has been suggested that dendritic bundles of ascending apical dendrites of cortical layer 5 pyramidal neurons form the center of cortical modules of vertically interconnected neurons which share functional properties (Mountcastle 1997; Peters and Sethares 1996). Labeling studies in both the visual and motor cortex showed that pyramidal neurons from the same bundle project to the same target, thereby supporting the idea that dendritic bundles are functionally related (Lev and White 1997; Vercelli et al. 2004). However, in another study it was shown that synaptic connectivity is independent of apical dendrite bundling (Krieger et al. 2007). Therefore, it is not very likely that dendritic bundles form the center of cortical modules and are the functional basis of a cortical microcircuit. Nevertheless, it has to be mentioned that other functional relations between pyramidal neurons within a dendritic bundle such as connectivity patterns between layer 2/3 and 5 pyramidal neurons within a bundle still need to be investigated. Although investigation about the functional relevance of dendritic bundles in the cortex is still ongoing, it is remains interesting to speculate about the functional consequences of alterations in apical dendrite bundling as observed in the current study in 5-HT_{3A} receptor knockout mice.

The fact that in 5-HT_{3A} receptor knockout mice the surface of these bundles is increased, suggests that connectivity between neurons has changed which could lead to alterations in information processing in the cortex of these mice.

However, if indeed alterations in information processing in 5-HT_{3A} receptor knockout mice would be observed, they might also be a consequence of the previously observed alterations in dendritic complexity of cortical layer 2/3 pyramidal neurons.

In conclusion, the results from the current study show that in the somatosensory cortex of 5-HT_{3A} receptor knockout mice, dendritic bundle size is different from wildtype mice. This finding, together with previously observed differences in dendritic complexity of cortical layer 2/3 pyramidal neurons and cortical reelin levels, suggests an important role for the 5-HT_3 receptor in determining the spatial organization of cortical connectivity in the mouse somatosensory cortex.

Acknowledgements

We would like to thank Erik Manders for his assistance in making the confocal images, Madhvi Nazir for assistance with the immunohistochemical stainings and David Julius (University of San Francisco, San Fransisco, CA) for providing the 5-HT_{3A} knockout mice.